ELSEVIER

Contents lists available at ScienceDirect

European Journal of Pharmaceutics and Biopharmaceutics

journal homepage: www.elsevier.com/locate/ejpb





Intradermal delivery of teriflunomide loaded emulsomes using hollow microneedles for effective minimally invasive psoriasis management

Mariam Zewail ^{a,*}, Haidy Abbas ^a, Nesrine El Sayed ^b, Heba Abd-El-Azim ^{a,c}

- a Department of Pharmaceutics, Damanhour University, Damanhour, Egypt
- ^b Department of Pharmacology and Toxicology, Faculty of Pharmacy, Cairo University, Cairo, Egypt
- ^c Postdoc Brigham and Women's Hospital, Harvard Medical School, Harvard University, United States

ARTICLE INFO

Keywords: Autoimmune diseases DMARDs Hollow microneedles Transdermal drug delivery

ABSTRACT

Conventional topical psoriasis treatments suffer from limited delivery to affected areas along with skin irritation due to high local drug concentration. Herein an attempt to improve the delivery of leflunomide's active metabolite (teriflunomide (TER)) by improving its solubility through nanoencapsulation in emulsomes (EMLs) besides ensuring effective intradermal delivery using hollow microneedles. Evaluation of colloidal characteristics of EMLs, encapsulation efficiency and drug release were performed. Additionally, the antipsoriatic activity in an imiquimod-induced psoriatic mouse model was evaluated by the measurement of inflammatory mediators' levels and histopathological assessment of anatomized skin. The particle size of the chosen EMLs formulation was 147.9 nm and the zeta potential value was -21.7. Entrapment efficiency was 97.23 % and EMLs provided sustained drug release for 48 h. No statistically significant differences in the *in vivo* levels of NF-KB, IL 8, MMP1, GSH, SOD and catalase between the animals treated by TER-EMLs and the negative control cohort were observed. Also, histopathological inspection of dissected skin samples reflected the superiority of TER-EMLs over TER suspension. Collectively, combining nanoencapsulation and hollow microneedles application improved TER properties and ensured effective TER delivery to the affected psoriatic areas.

1. Introduction

Psoriasis is reported to be a widely spread autoimmune skin disease featuring high epidermal proliferation and increased dermal inflammation. Psoriatic skin lesions are mostly scaly, red, sharply detached and hardened plaques. Psoriasis affects about 3 % of the general population. Despite no age exemption, young and middle-aged adults represent the highest affected categories among psoriasis patients [1]. Psoriasis significantly impairs both the quality and expectancy of the affected patients' lives. It may lead to depression and social stigma [2]. Also, psoriasis has been linked to cardiovascular diseases and lymphoma [3].

Psoriasis has a major genetic component, with heritability estimated to be 60–90 % [4]. However, it is thought that other factors like smoking, air pollutants, skin infections, alcohol, drugs and emotional stress could trigger the initiation of that torturing disease [1,2]. Also, oxidative stress is thought to contribute to the prognosis of psoriasis [1]. Plaque psoriasis and psoriasis vulgaris are the most frequent kinds of psoriasis. Additionally, psoriasis includes pustular, erythrodermic, inverse, guttate, scalp and nail psoriasis [3,5].

Psoriasis can be managed by topical, systemic medications or phototherapy depending on the severity of the disease [6]. Topical medications containing synthetic vitamin D3 analogues, corticosteroids, retinoid derivatives or anthralin may be utilized. On the other hand, systemic medications include calcineurin inhibitors, immunosuppressive medications, acitretin and isotretinoin.

Prolonged administration of systemic treatments is associated with several side effects [7] while the conventional topical delivery of anti-psoriatic agents with high doses may suffer from limited delivery to affected areas of skin along with skin irritation due to high local drug concentration [6].

Nanocarriers can overcome the limitations of conventional psoriasis treatment as they improve drug solubility, stability, bioavailability, and penetration through skin layers hence the pharmacological effects of drugs are improved [6]. Lipid-based nanocarriers can be used to achieve effective topical and transdermal drug delivery. They have low toxicity, better thermal stability compared with other types of nanocarriers and can be easily prepared on a large scale [6].

Among lipid-based nanocarriers are emulsomes (EMLs) which are

E-mail addresses: mariamzewail@pharm.dmu.edu.eg, mariamzewail@gmail.com (M. Zewail).

^{*} Corresponding author.

lipid-based vesicles typically composed of a phospholipid bilayer surrounding a solid lipid core. It merges the advantages of both liposomes and nanoemulsions. The phospholipid bilayer aids in the stabilization of EMLs' structure with no need for surfactant addition. The solid lipid core increases the solubilization of poorly soluble drugs, increases drugs' loading efficiency and provides extended drug release [8].

Another approach to ensure effective drug delivery in psoriasis is the use of microneedle (MN) technology. A MN patch represents an array of arranged micron-size pointed projections [9]. MNs are a rapidly emerging drug delivery technology due to their potential to painlessly penetrate the skin and deliver compounds directly to the desired site [9]. Additionally, MNs showed high potential for prolonged and controlled delivery of drugs, effective transdermal and intradermal medication availability, the possibility of treatment cessation, providing high localized drug accumulation, reducing dosage regimen, overcoming needles' phobia and providing non-invasive self-administration [10,11]. Thus, recently, researchers have explored the MNs' applications for the delivery of tacrolimus [12] and calcipotriol [13] for the treatment of psoriasis as a promising therapeutic approach.

In particular, hollow MNs (Ho-MNs) are fabricated to have a central or off-central pore in their tip. Those holes act as direct micro-openings in the dermal layers permitting the drug to flow into the skin layers [14]. In turn, this modality would allow for steep drug diffusion and promote local drug concentration leading to superior localized pharmacological productiveness [10]. Ho-MNs are advantageously characterized by securing accurate adjustable doses and controlling drug delivery rates without restrictions on the drug formulation being administered [9,15]. For instance, considering psoriasis management, resin Ho-MNs proved highly efficient in delivering methotrexate to psoriatic skin successfully [16].

Leflunomide (LEF) belongs to disease-modifying antirheumatic drugs (DMARD) that can be used as a monotherapy in both psoriatic arthritis and rheumatoid arthritis treatment. Besides, LEF was proven to have a positive effect on psoriasis treatment. Post-marketing studies have revealed that treatment with LEF has pharmacological effects resembling those of methotrexate and superior to other DMARDs [17]. Kaltwasser et al. [18] reported that leflunomide has proven clinical efficacy in one hundred ninety patients having psoriatic arthritis and active psoriasis [18]. Also, Nash et al.[19] reported that leflunomide has manifested a promise in the therapeutic outcomes of human plaque psoriasis and psoriatic arthritis [19].

Teriflunomide (TER) (A77-1726) which is the active (LEF) metabolite can inhibit de novo pyrimidine synthesis due to selective inhibition of a dihydroorotase dehydrogenase [20]. TER leads the actively proliferating T cells and B lymphocytes to undergo cell cycle arrest through inhibition of clonal expansion. Besides, TER has anti-inflammatory and immunomodulatory properties that may be attributed to the reduction of nuclear factor KB-dependent gene transcription, tumor necrosis factor-induced nuclear factor KB activation, production of cell adhesion molecules, and protein kinases [21].

Prolonged systemic administration of LEF and its metabolite (TER) has been reported to cause several adverse effects including immune suppression, elevated liver enzyme levels, gastrointestinal symptoms and cytopenia [20,22–24].

The main aim of the current study is to present an effective minimally invasive method for psoriasis treatment with reduced side effects. To attain this, TER-loaded EMLs were prepared and *in vitro*, characterization of the prepared carriers was performed. The selected EMLs were administered to mice with an imiquimod-induced psoriasis model through a transdermal route using hollow MNs to ensure effective transdermal drug delivery.

To our knowledge, this is the first report for the administration of TER-loaded EMLs for psoriasis management through intradermal delivery using Ho-MNs.

2. Materials

Compritol was kindly gifted by Gattefosse (Saint-Priest, France). Lipoid S 100 was a kind gift from Lipoid (Ludwigshafen, Germany). Cholesterol was obtained from Sigma-Aldrich (Steinem, Germany). Teriflunomide was supplied from MedKoo Biosciences (North Carolina, USA). AdminPenTM hollow microneedle arrays were obtained from NanoBioSciences LLC, USA. The rest of the chemicals and reagents are analytical grade.

3. Methods

3.1. Development of TER-loaded EMLs

Preparation of EMLs was performed following the procedure described previously by Abbas et al. [25] with slight modifications. Compritol, Lipoid S 100 and cholesterol were dissolved in a sufficient amount of dichloromethane in a ratio of (1: 1.2: 0.4) and kept at 50 $^{\circ}$ C on the magnetic stirrer till complete evaporation of the organic solvent and thin film formation. The formed film was rehydrated using deionized water and subjected to 3 ultrasonication cycles (SonicaR 2200 EP S3, Soltec, Milan, Italy) each one is 5 min at 60 mA. The formed dispersion was kept in the refrigerator for further investigation.

For the preparation of TER-loaded EMLs, different amounts of TER (5, 10 and 15 mg) were dissolved in dichloromethane along with the lipid phase. Then the following steps were carried out according to the same procedure that was used for the preparation of blank EMLs.

3.2. Intradermal application using AdminPen $^{\text{TM}}$ hollow microneedles array

Full-thickness human skin was intact and collected after abdominal plastic surgery by a male volunteer. Briefly, following the removal of subcutaneous fats, the upper skin surface was cleaned with normal saline solution, dried, securely sheathed and preserved at $-20\,$ °C until further need. The previously outlined optimized conditions for preserving human skin for 3–6 months were followed in this protocol [26]. AdminPen^TM, 43 stainless steel metallic Ho-MNs array of 1200 μm length was used to intradermally inject both free TER and EMLs encapsulating TER into the exterior surface of the cleansed skin following the thumb and index finger strategy.

3.3. Particle size and zeta potential measurements

At a scattering angle of 173° and 25° C, Zeta sizer Nano ZS (Malvern Instrument, UK) was employed to determine the following colloidal parameters; average particle size, polydispersity index (PDI), and zeta potential values.

3.4. Entrapment efficiency (EE%)

Indirect evaluation of entrapment efficiency was performed using a Centrisart®-I tube (MWCO 300 kDa, Sartorius AG, Gottingen, Germany). First, TER-EMLs were centrifugated at 5000 rpm for 30 min to discrete free unentrapped TER. Second, the concentration of free TER was analyzed using HPLC connected to a UV detector at 305 nm [20].

$$\textit{EE}(\%) = \frac{\textit{TotalTER} concentration - concentration of unencapsulated TER}{\textit{TotalTER} concentration} \\ \times 100$$

3.5. Transmission electron microscope (TEM)

A transmission electron microscope (TEM; JEM-100CX; JEOL, Japan) was used to examine the morphology of selected TER-EMLs formulation after staining with uranyl acetate.

3.6. In vitro drug release and release kinetics

Dialysis technique was used to study the *In vitro* drug release profile of selected TER-EMLs. Initially, for each sample, 500 μg of TER-EMLs was put in a dialysis bag and submerged in 75 ml of PBS (pH 7.4), to attain sink conditions, under shaking at 37 \pm 0.2 °C and 100 rpm [20]. Then, samples were withdrawn, at predetermined time points, and compensated with fresh media. Following that, an HPLC method was used to assess the amount of TER released using UV detection at 305 nm [20]. Samples were measured in triplicates. Different mathematical release models including zero order, first order, Higuchi and Korsmeyer Peppas were used to estimate release data fitting and R^2 values determination using DD solver software (an Excel add-in).

3.7. Stability study

The selected TER-EMLs were monitored for particle size, entrapment efficiency and PDI throughout 3 months of storage at 4 $^{\circ}$ C.

3.8. Ex vivo insertion properties of AdminPen $^{\text{TM}}$ hollow microneedles array

The quality of skin penetration using AdminPen™ Ho-MNs was evaluated as previously reported with proper changes [14]. According to the insertion protocol detailed in Section 3.2, the MNs were applied to the skin, and then digital images were snapshot for the skin after MNs removal using Samsung Galaxy Note8, dual pixel, 12 MP, PDAF. The count of visually clear pores formed by Ho-MNs was determined and subsequently, the percentage of percutaneous penetration was also deduced based on the following equation:

$$\label{eq:theorem} \textit{The percentage of penetration} = \frac{\textit{Number of created holes in skin}}{\textit{Total number of hollow microneedles}} \times 100$$

3.9. In vivo studies

3.9.1. Animals

Thirty-two female BALB/c mice weighing 18–22 gm were obtained from National Organization Center, Giza, Egypt. Mice were housed under constant temperature (25 $^{\circ}$ C), humidity, and alternating 12 h light and dark cycles. A standard diet and free water supply will be allowed throughout the experimental study. The current study was carried out by the US National Institutes of Health's Guide for the Care and Use of Laboratory Animals (NIH Publication No. 85–23, revised 2011), which was approved by the Research Ethics Committee of the Faculty of Pharmacy, Cairo University, Cairo, Egypt (Ethical approval no. PT 3271). All necessary steps were taken to reduce animal suffering during the experiment schedule.

3.9.2. Experimental design

Animals were randomly divided into four groups (n = 8); Group I: (Negative control) mice received normal saline. Psoriasis was induced in Groups II, III and IV according to the study previously described by Elgewelly et al. [27,28] through the daily application of 62.5 mg of Imiquimod cream (ALDARA® cream 5 %) on the shaved back of mice (2.5cmx2cm). Group II received normal saline and was kept as a positive control group. On the other hand, groups III and IV received TER suspension and TER-EMLs through intradermal injection by hollow MNs. Treatments were commenced on the shaved back skin after 4 h of IMQ cream application and the experiment was extended for 7 days. On the eighth day, animals were sedated with a ketamine (100 mg/kg)/xylazine (10 mg/kg) combination, and blood samples were taken from the retro-orbital sinuses of all mice before being humanely terminated by cervical dislocation. Eventually, for histopathological investigations, the back dorsal skin (n = 3/group) was shaved and fixed in 10 % formalin. Fig. 1 illustrates a schematic diagram for the in vivo experiment.

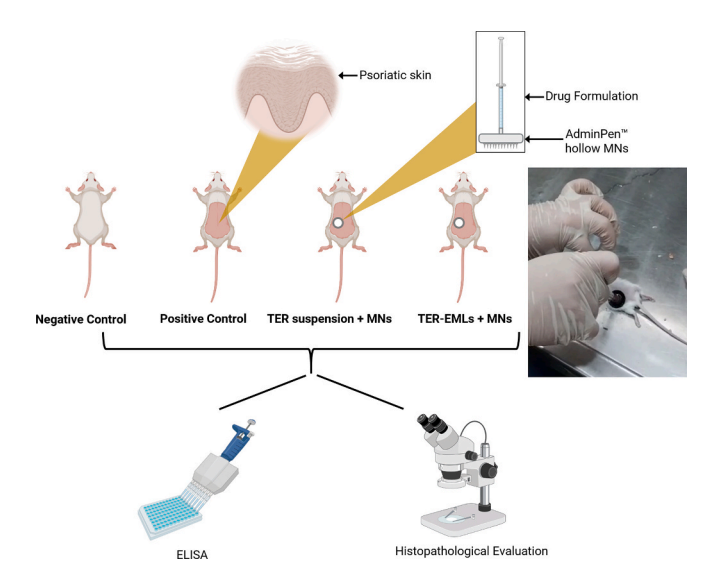


Fig. 1. Schematic representation showing the different treatment groups investigated in the *in vivo* study and further characterization techniques. Intradermal administration of TER formulations using AdminPenTM hollow MNs into the psoriatic lesion in mice.

3.9.3. Enzyme-linked immunosorbent assay (ELISA)

From *retro*-orbital sinus, blood samples were collected and centrifuged at 1000xg for 20 min to separate clear sera that were utilized for ELISA assay. Quantitative determination of the serum levels of interleukin 8 (IL 8), Glutathione S transferase (GSH), catalase, superoxide dismutase (SOD), matrix metalloproteinases 1 (MMP1) and nuclear factor kappa B (NF-KB) were evaluated using ELISA kits (Glory Science Co, Ltd, USA). All procedures were done according to the manufacturers' procedures.

3.9.4. Histopathological examination

Before commencement with the histopathological examination, anatomized skin tissue samples of mice of different experimental groups were fixed in 10 % (v/v) neutral buffered formalin for 72 h. briefly, dissected tissue sections were first trimmed, treated with ethanol, and soaked in xylene before infiltration with synthetic paraplast tissue embedding media. Samples (5μ) were finally stained with hematoxylin and eosin for light microscopy imaging.

3.10. Statistical analysis

Data are recorded as mean \pm SD. All statistical analysis were carried out using Prism 7 software. Results of ELISA were analysed by One-way ANOVA (p < 0.0001), and colloidal characteristics of nanocarriers were analysed by student's *t*-test (p < 0.05).

4. Results and discussion

4.1. Colloidal characteristics of blank and TER-loaded EMLs

Blank and TER-loaded EMLs were prepared by the thin film hydration method as previously described by Rizk et al. [29] and Abbas et al. [25]. EMLs were primarily chosen to match the physicochemical characteristics of TER as it possesses a hydrophobic nature. EMLs are reported to increase the solubility of lipophilic drugs and sustain their release period [30,31]. Also, EMLs possess the characteristics of both emulsions and liposomes that permit their accommodation to higher amounts of drugs compared with the aforementioned delivery systems [32,33]. The inclusion of cholesterol and compritol in the formulation of EMLs was attributed to their ability to enhance the loading efficiency of EMLs besides the ability of cholesterol to increase the stability of lipoid

S's phospholipid layer [34].

As Table 1 illustrates, the size of prepared formulations ranged between 120.7 to 159.8 nm. TER loading had a significant effect on increasing particle size from 120.7 to 135.3,147.9 and 159.8 nm in F1 (blank) and TER-loaded EMLs F2, F3 and F4, respectively. The particle size increased from 135.3 to 159.8 nm when the TER concentration increased from 5 to 15 mg. EMLs had uniform size distribution as PDI values were 0.4 or less indicating nanodispersion homogeneity. PDI values mirror the degree of nanodispersion homogeneity, estimations closer to zero reflect a more uniform dispersion [35,36].

The surface charge of nanocarriers is considered an important factor in preserving the stability of the prepared nanodispersion. High surface alterations initiate repulsive forces that counteract particle aggregation [37–39]. The prepared EMLs carried a negative surface charge between -20.5 and -22 (Table 1). The highest nanocarriers' stability is attained with zeta potential values of approximately $\pm~30\,$ mV therefore the prepared EMLs are considered stable [40–42]. Our findings are along with previously reported results [25,29].

4.2. EE %

The EE % of F2, F3 and F4 were 96.78, 97.23 and 97.94, respectively as listed in Table 1. This high EE % may be referred to the potential of EMLs to improve the encapsulation efficiency of hydrophobic drugs [25,29] as they are composed of a mixture of lipoid S, compritol and cholesterol.

4.3. TEM

TEM micrograph of F3 (selected EMLs formulation) as illustrated in Fig. 2, showed a smooth spherical structure. The absence of drug crystals in the micrograph indicates the good encapsulation of TER in EMLs.

4.4. In vitro drug release and release kinetics

TER release from different EMLs dispersions exhibited a biphasic release sketch that lasted for 48 h as shown in Fig. 3. Increasing TER amount in EMLs formulations from F2 (5 mg) to 10 mg in F3 and 15 mg in F4 resulted in an increasing burst effect during the first hour from 12.3, 14 and 17.6 % respectively. The observed burst effect could be attributed to the adsorption of TER on the vesicles' surface and the interphase in the bilayered phospholipid shell [25]. The sustained release profile could be related to the time required by TER to diffuse from the EMLs' matrix and the concentration gradient between the EMLs and the release medium [43]. Different EMLs formulations showed a release pattern faster than TER suspension. This could be explained by the impact of nanoencapsulation on enhancing drug solubility and hence, their *in vitro* release occurs at a higher rate [36,44].

Upon applying zero, first, Higuchi and Korsmeyer Peppas models to release data. Korsmeyer Peppas had the highest R^2 values, as Table 2 illustrates, with n values below 0.45 indicating that EMLs obeyed the

 $\begin{tabular}{ll} \textbf{Table 1} \\ \textbf{Particle size, PDI, zeta potential and EE \% of different EMLs formulations.} \\ \end{tabular}$

Formulation	TER concentration	Particle size (nm)	PDI	Zeta potential (meV)	EE %
F1		$120.7 \pm \\1.3$	$\begin{array}{c} 0.278 \\ \pm \ 0.12 \end{array}$	$-~20.5~\pm\\0.67$	
F2	5 mg	$135.3 \pm \\2.16$	$\begin{array}{c} 0.355 \\ \pm \ 0.45 \end{array}$	$-~20.7~\pm\\0.56$	96.78 ± 1.23
F3	10 mg	$147.9 \pm \\ 0.98$	$\begin{array}{c} 0.270 \\ \pm \ 0.23 \end{array}$	$-21.7 \pm \\0.98$	97.23 \pm 0.98
F4	15 mg	$159.8 \pm \\1.12$	$\begin{array}{c} 0.422 \\ \pm \ 0.87 \end{array}$	$-22~\pm$ 0.87	97.94 \pm 0.78
F3 Stability	10 mg	$143.4 \pm \\1.34$	$\begin{array}{c} 0.362 \\ \pm \ 0.65 \end{array}$	$-\ 21.5\ \pm\ 0.45$	97.14 ± 0.54

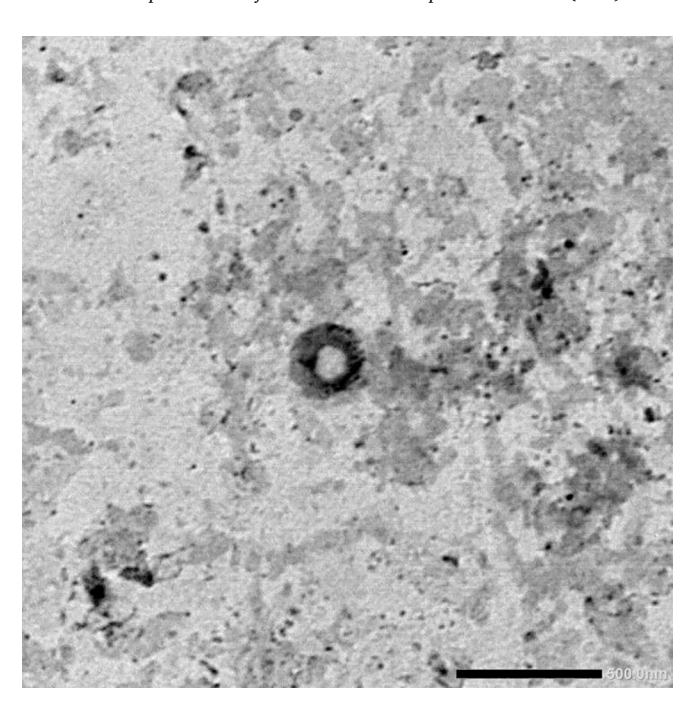


Fig. 2. TEM micrograph of selected TER EMLs formulation.

Fickian diffusion pattern. Moreover, the drug diffusion process marked the most prominent drug release mechanism [45].

From colloidal characteristics and in vitro release results F3 was selected for further investigation as its size was 147.9 nm with a low PDI value (0.270), high EE (97.23 %) and possessed sustained release profile.

4.5. Stability

The selected EMLs formulation (F3) showed good stability upon storage in the refrigerator for 3 months with no statistically significant variations from the freshly prepared formulation in particle size and EE % (Student's *t*-test; p < 0.05).

4.6. AdminPen TM hollow microneedle array ex vivo insertion characteristics

The minimally invasive AdminPenTM Ho-MNs arrays are designed to achieve intradermal or transdermal delivery of liquid dispersions as detailed in the US Patent No. 7,658,728 [46]. This MN array was designed with an innovative structure consisting of 43 sharp-edged MN shafts; each is 1200 μ m in height having an off-centred hollow pore on its side, to avoid needle blockage while allowing for efficient and continuous drug flow. Microholes of about 1100 to 1200 μ m in depth are created in both the stratum corneum and epidermis layers upon application of the AdminPenTM device [14,47]. Soon after the removal of MNs, the formed micropores simply cave in and the skin barrier is shortly re-established avoiding any possible skin infection risk [14]. Based on the aforementioned benefits, AdminPenTM Ho-MNs were carefully chosen to deeply deliver the formulated TER-EMLs through skin layers.

The performance of MNs is determined by their insertion efficiency, as the stratum corneum should be efficiently pierced for the MN array to exert its effect [48]. Simply, effective skin penetration via AdminPenTM Ho-MNs is pivotal for efficient TER-EMLs transdermal delivery. Excised skin samples and Parafilm M® membrane can be used as skin models to assess the penetration capabilities of MNs [14,48]. As a part of an earlier study, the author, Abd-El-Azim [14], showed the successful insertion of the presently-utilized AdminPenTM Ho-MNs through Parafilm M®

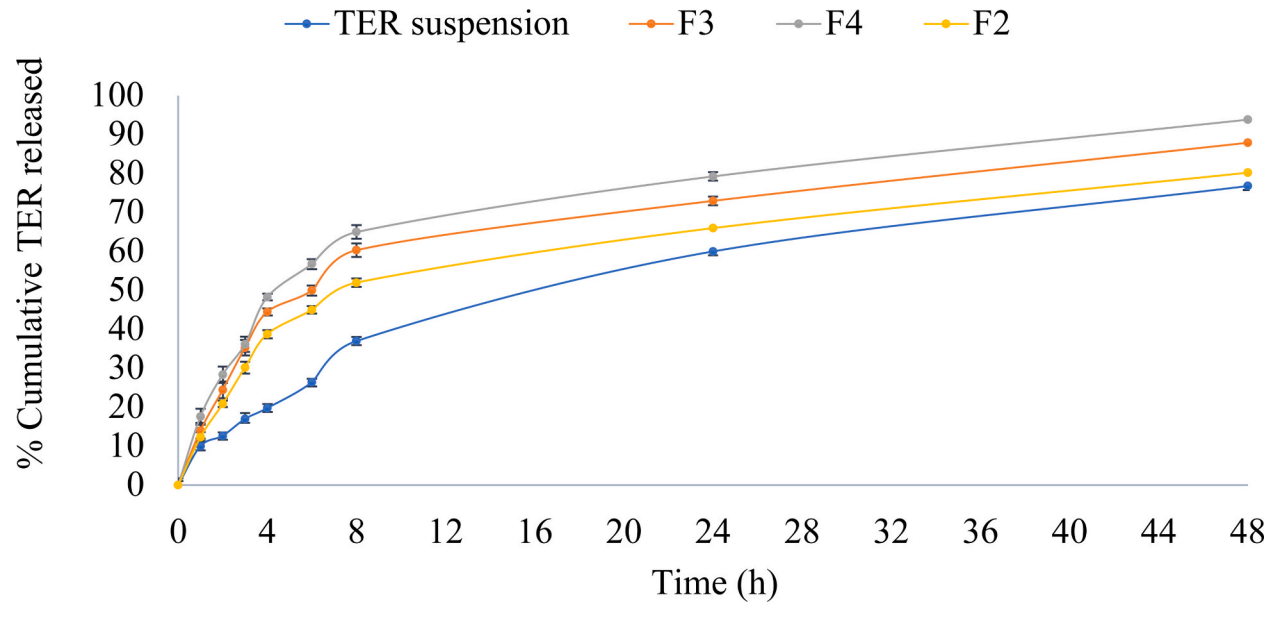


Fig. 3. In vitro drug release for TER suspension and TER EMLs formulations.

Table 2 Release kinetics.

Model	R ²					
	TER suspension	F2	F3	F4		
Zero order	0.889	0.715	0.687	0.675		
First order	0.971	0.865	0.906	0.950		
Higuchi	0.980	0.860	0.837	0.958		
Korsmeyer Peppas	0.988	0.984	0.981	0.979		

membrane recording a penetration depth of 889 µm equivalent to more than 80 % of the height of the actual needle. According to literature, excised human skin was proven to be the "gold standard" in *in vitro* testing [49]. In this work, excised human skin was used to evaluate the insertion potentials of the AdminPenTM hollow MNs. As shown in Fig. 4, the generated images reflected complete insertion producing 43 dermal micropores representing the 43 MNs in the array with clear interspaces. These results proved effective skin penetration and demonstrated the strong mechanical strength of the utilized MNs. Accordingly, the anticipated MN-EMLs combined delivery approach untied an encouraging potential for the deep effective TER to psoriatic lesions.

4.7. In vivo studies

The previously effective imiquimod-induced mouse model was followed for psoriasis induction [27,50–52]. This model was chosen because of its capacity to replicate several human plaque-type psoriatic inflammatory features such as skin thickness, erythema, scaling, parakeratosis, neo-angiogenesis, and acanthosis. In addition to neutrophils, T cells, and dendritic cells, there is an inflammatory presence of dendritic cells [50]. Animals were split into four groups; negative control, positive control, TER suspension using AdminPenTM Ho-MNs and TER-EMLs using AdminPenTM Ho-MNs.

4.7.1. ELISA

The underlying triggering factor of the hyperproliferation of keratinocytes in psoriasis is still unclear however, it could be related to autocrine stimulation of epidermal group factor by transforming growth factor-alpha and interleukins like IL-8 [53]. NF-KB is a crucial player in the pathogenesis of psoriasis. It is a protein transcription factor that regulates inflammation and immune responses. Elevated levels of active phosphorylated NF-KB are characteristic of psoriasis [54]. Activation of NF-KB has been linked to high levels of different inflammatory mediators and genes like MMP1 and MMP9 [55]. NF-KB is upregulated in psoriatic patches and response to treatment [56].

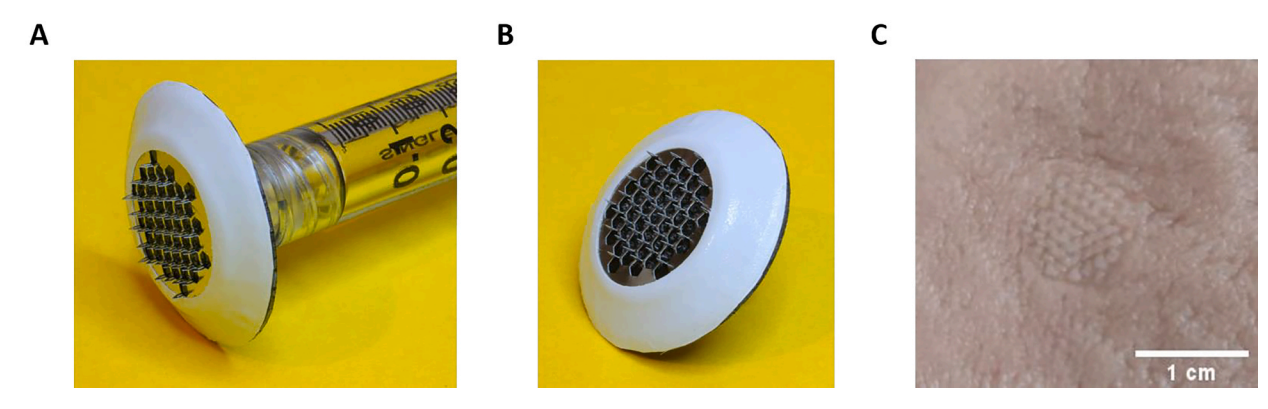


Fig. 4. A & B) AdminPenTM hollow MNs showing 43 stainless-steel MN shafts of 1200 μm in length and 1 cm² in area (Image was used with permission from AdminMed). C) Image recorded by a standard mobile camera (Samsung Galaxy Note8, 12 MP, dual pixel, PDAF) illustrating excised full-thickness human skin after insertion of AdminPenTM 1200 μM Ho-MN array.

Also, oxidative stress has a major role in the development and severity of psoriasis [57]. Psoriasis onset is related to the activity of SOD and glutathione peroxidase in erythrocytes [57]. In addition, GSH plays an anti-inflammatory role in controlling the proliferation of keratinocytes.

Levels of NF-KB, MMP1, GSH, SOD, IL8 and catalase were determined at the end of the experiment as illustrated in Fig. 5. Overall levels of MMP1, NF-KB, and IL8 are elevated in the positive control group compared with the untreated control group. On the other hand, levels of SOD, catalase and GSH are lower in the positive control group in contrast to the negative control group. These findings are along with the previous results of the levels of these inflammatory markers in psoriasis patients [58,59].

NF-KB level was increased by 4.8 and 2.1 folds in the positive control group and the group received TER suspension. On the other hand, KF-KB was 0.95 and 1.03 ng/g tissue in the negative control group and TER-EMLs group, respectively. These findings could be associated with the ability of TER to suppress NF-KB dependent gene transcription, tumor necrosis factor–induced activation of nuclear factor KB, and expression of protein kinases and cell adhesion molecules [21].

Levels of IL8 increased by 3, 1.95 and 1.3 folds in the positive control group, TER suspension group and TER-EMLs group compared with the untreated control group. Also, levels of MMP1 were 3.4, 1.84, 1.56 and 1.4 ng/g tissue in the positive control group, TER suspension group, and TER-EMLs group in the negative control group, respectively. Levels of MMP1 are usually elevated in psoriasis patients.

Levels of GSH were 4.9, 4.7, 2.2 and 1.34 pg/g tissue in the negative control group, TER EMLs group, TER suspension group and the positive

control group, respectively. Levels of SOD decreased by 5.6, 2.11 and 1.27 folds in the positive control group, TER suspension group and TER-EMLs group, respectively compared with the untreated control group.

4.7.2. Histopathological examination

As Fig. 6 demonstrates, the negative control group revealed normal histological skin structure. On the contrary, the positive control group section manifested increasing thickness of the epidermal layer (arrow head) covered by serocellular crust (star) with congestion of dermal blood vessels (black arrow) and infiltration of the dermis by mononuclear inflammatory cells (red arrow). This indicated the effectiveness of psoriasis induction as psoriasis is distinguished by epidermal hyperplasia and the presence of inflammatory infiltrates that are composed of neutrophils, dermal dendritic cells, T cells and macrophages [56].

Concerning the treatment groups, TER suspension in the MNs group demonstrated parakeratosis formation (star) with increasing thickness of the epidermal layer (arrowhead). On the contrary, the group treated with TER-EMLs in MNs showed only infiltration of the dermis by mononuclear inflammatory cells (arrow).

Interestingly, the results of ELISA are in harmony with the histopathological examination findings. Improvement of psoriasis in TER suspension and TER-EMLs in MNs may be attributed to two reasons. First, the use of Ho-MNs ensured effective deep transdermal delivery of TER suspension and TER-EMLs allowing for high drug localization at the target psoriatic lesion. The second reason is the ability of TER to inhibit TNF α action by hindering IkB-degradation and thereby prohibiting the release of NF-KB [60]. Also, TER can reduce the proliferation of T and B lymphocytes [21]. The superior effect of the TER-EMLs group over the

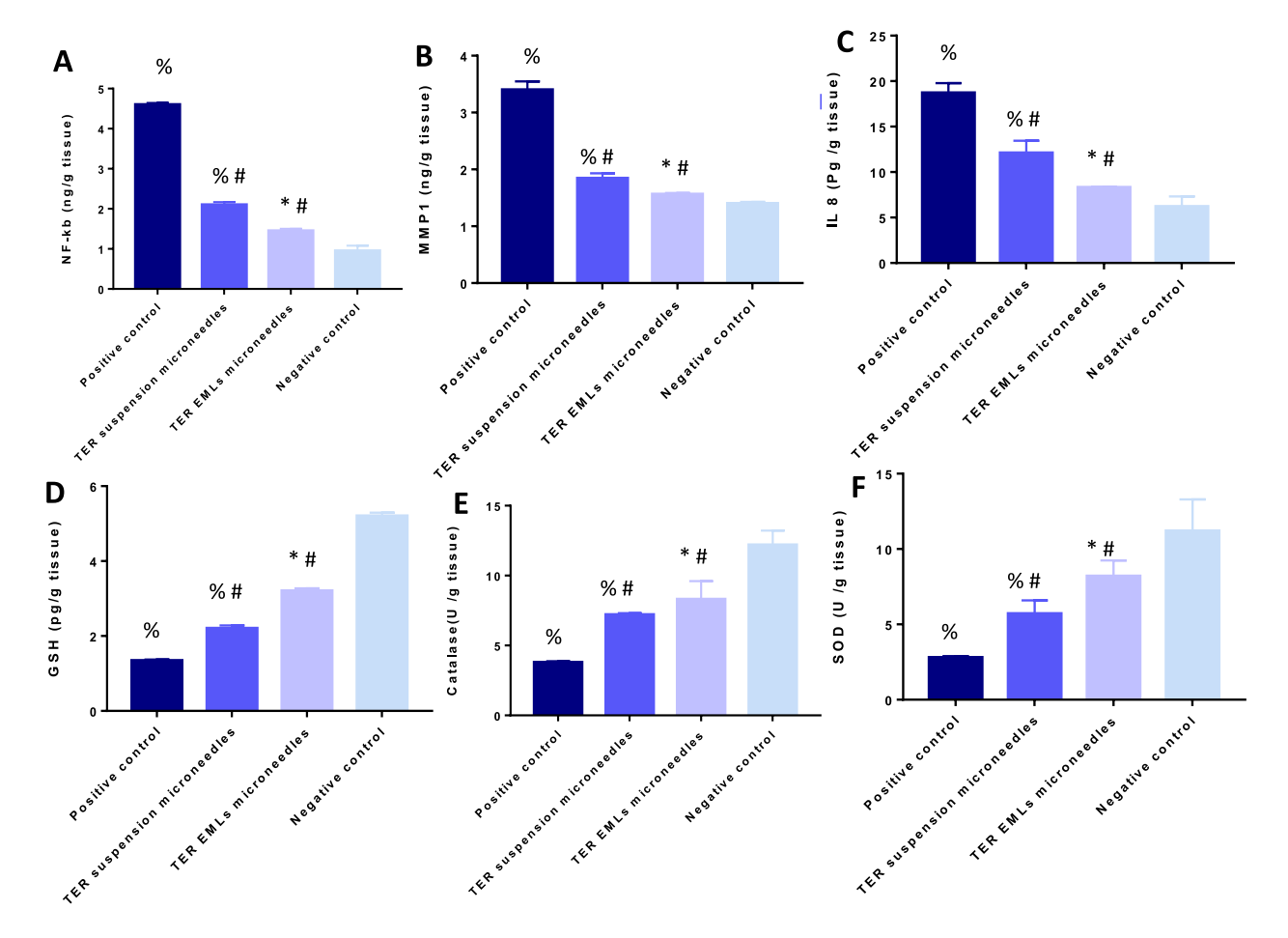


Fig. 5. Serum levels of NT-kb, MMP1, IL8, GSH, catalase and SOD of different experimental groups at the end of the experiment. Data analysis was conducted using one-way ANOVA followed by Tukey's test (p < 0.0001). % significant from the negative control group. # significant from the negative control group. * significant from TER suspensions in microneedles.

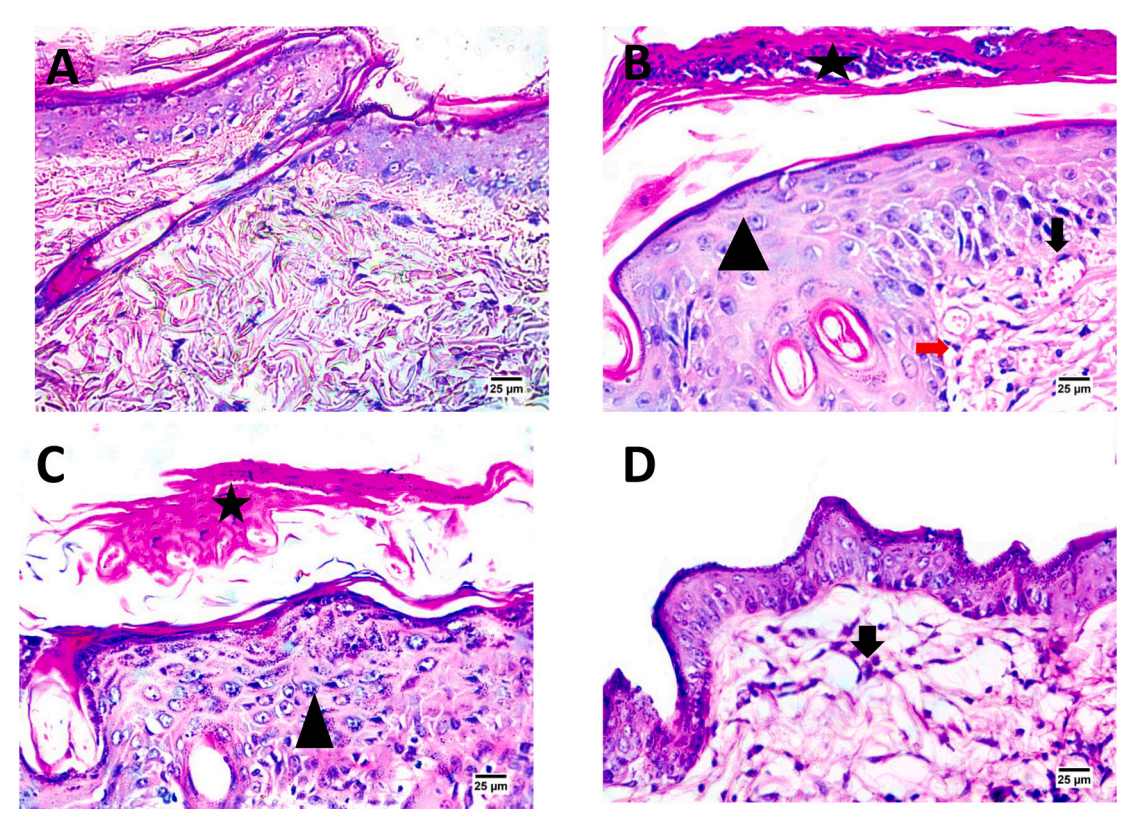


Fig. 6. Photomicrographs of skin dissected from different experimental groups at the end of the experiment using hematoxylin and Eosin stain. (A) Negative control, (B) positive control, (C) TER suspension group in microneedles group and (D) TER EMLs in microneedles group.

TER suspension group could be credited to the impact of encapsulation on boosting the solubility and, thus, the pharmacological effects of TER. These findings are to the outcomes reported by Abbas et al.[25] and Zewail et al.[20] who reported that nanoencapsulation of LEF and TER resulted in a significant improvement in their pharmacological effects in rheumatoid arthritis management. These findings validated our hypothesis concerning the synergistic capabilities of using Ho-MNs for effective intradermal delivery of TER-EMLs to achieve enhanced therapeutic outcomes against psoriasis.

5. Conclusion

This study unveils additional insights into the employment of EMLs and Ho-MNs. Initially, spherical TER-loaded EMLs were successfully formulated with smooth surfaces and possessed uniform distribution and high entrapment efficiency. Moreover, EMLs provided a sustained release profile. Furthermore, the skin insertion test confirmed that AdminPen™ Ho-MNs successfully pierced the stratum corneum for the delivery of their cargo. Importantly, in vivo, results in imiquimodinduced mice revealed the superiority of TER-EMLs over TER suspension after intradermal administration using AdminPen™ Ho-MNs. This was manifested by non-significant differences in inflammatory mediators' levels in the group received TER-EMLs and the negative control group and was further confirmed by histopathological examination of dissected skin samples. These findings suggested the effectiveness of the presented EMLs Ho-MNs combined non-invasive delivery strategy to effectively treat psoriasis. Potentially, MNs and EMLs modality could present a promising core in the upcoming generation of anti-psoriatic drug delivery systems.

CRediT authorship contribution statement

Mariam Zewail: Writing – review & editing, Writing – original draft, Software, Methodology, Investigation, Data curation,

Conceptualization. **Haidy Abbas:** Visualization, Validation, Supervision, Software, Methodology, Data curation, Conceptualization. **Nesrine El Sayed:** Validation, Supervision, Resources, Formal analysis, Data curation, Conceptualization. **Heba Abd-El-Azim:** Writing – original draft, Validation, Software, Resources, Methodology, Data curation, Conceptualization.

Declaration of competing interest

The authors declare that they have no known competing financial interests or personal relationships that could have appeared to influence the work reported in this paper.

Data availability

No data was used for the research described in the article.

References

- [1] V.M. Pujari, S. Ireddy, I. Itagi, The serum levels of malondialdehyde, vitamin e and erythrocyte catalase activity in psoriasis patients, J. Clin. Diagn. Res. 8 (11) (2014) CC14.
- [2] E.-C. Dobrică, M.-A. Cozma, M.-A. Găman, V.-M. Voiculescu, A.M. Găman, The involvement of oxidative stress in psoriasis: a systematic review, Antioxidants 11 (2) (2022) 282.
- [3] N. Weigle, S. McBane, Psoriasis, Am. Fam. Physician 87 (9) (2013) 626.
- [4] A. Raharja, S.K. Mahil, J.N. Barker, Psoriasis: a brief overview, Clin. Med. 21 (3) (2021) 170.
- [5] J.P. Rajguru, D. Maya, D. Kumar, P. Suri, S. Bhardwaj, N.D. Patel, Update on psoriasis: a review, J. Family Med. Primary Care 9 (1) (2020) 20.
- [6] U.U.M. Nordin, N. Ahmad, N. Salim, N.S.M. Yusof, Lipid-based nanoparticles for psoriasis treatment: a review on conventional treatments, recent works, and future prospects, RSC Adv. 11 (46) (2021) 29080–29101.
- [7] R. Lai, D. Xian, X. Xiong, L. Yang, J. Song, J. Zhong, Proanthocyanidins: novel treatment for psoriasis that reduces oxidative stress and modulates Th17 and Treg cells, Redox Rep. 23 (1) (2018) 130–135.
- [8] H.M. Aldawsari, S.M. Badr-Eldin, N.Y. Assiri, N.A. Alhakamy, A. Privitera, F. Caraci, G. Caruso, Surface-tailoring of emulsomes for boosting brain delivery of

- vinpocetine via intranasal route: in vitro optimization and in vivo pharmacokinetic assessment, Drug Deliv. 29 (1) (2022) 2671–2684.
- [9] W. Zhang, W. Zhang, C. Li, J. Zhang, L. Qin, Y. Lai, Recent advances of microneedles and their application in disease treatment, Int. J. Mol. Sci. 23 (5) (2022) 2401.
- [10] J. Wang, J. Zeng, Z. Liu, Q. Zhou, X. Wang, F. Zhao, Y. Zhang, J. Wang, M. Liu, R. Du, Promising strategies for transdermal delivery of arthritis drugs: microneedle systems, Pharmaceutics 14 (8) (2022) 1736.
- [11] E. Larraneta, R.E. Lutton, A.D. Woolfson, R.F. Donnelly, Microneedle arrays as transdermal and intradermal drug delivery systems: materials science, manufacture and commercial development, Mater. Sci. Eng. R. Rep. 104 (2016) 1–32.
- [12] Q. Wang, X. Qin, J. Fang, X. Sun, Nanomedicines for the treatment of rheumatoid arthritis: state of art and potential therapeutic strategies, Acta Pharm. Sin. B 11 (5) (2021) 1158–1174.
- [13] L. Liang, W.M. Fei, Z.Q. Zhao, Y.Y. Hao, C. Zhang, Y. Cui, X.D. Guo, Improved imiquimod-induced psoriasis like dermatitis using microneedles in mice, Eur. J. Pharm. Biopharm. 164 (2021) 20–27.
- [14] H. Abd-El-Azim, I.A. Tekko, A. Ali, A. Ramadan, N. Nafee, N. Khalafallah, T. Rahman, W. Mcdaid, R.G. Aly, L.K. Vora, Hollow microneedle assisted intradermal delivery of hypericin lipid nanocapsules with light enabled photodynamic therapy against skin cancer, J. Control. Release (2022) 849–869.
- [15] J. Yang, X. Liu, Y. Fu, Y. Song, Recent advances of microneedles for biomedical applications: drug delivery and beyond, Acta Pharm. Sin. B 9 (3) (2019) 469–483.
- [16] Y. Ren, J. Li, Y. Chen, J. Wang, Y. Chen, Z. Wang, Z. Zhang, Y. Chen, X. Shi, L. Cao, Customized flexible hollow microneedles for psoriasis treatment with reduced-dose drug, Bioeng. Transl. Med. (2023) e10530.
- [17] P.B. Jones, D.H. White, Reappraisal of the clinical use of leflunomide in rheumatoid arthritis and psoriatic arthritis, Open Access Rheumatol. (2010) 53–71.
- [18] J.P. Kaltwasser, P. Nash, D. Gladman, C.F. Rosen, F. Behrens, P. Jones, J. Wollenhaupt, F.G. Falk, P. Mease, Efficacy and safety of leflunomide in the treatment of psoriatic arthritis and psoriasis: a multinational, double-blind, randomized, placebo-controlled clinical trial, Arthritis & Rheumatism: Off. J. Am. College Rheumatol. 50 (6) (2004) 1939–1950.
- [19] P. Nash, D. Thaçi, F. Behrens, F. Falk, J.P. Kaltwasser, Leflunomide improves psoriasis in patients with psoriatic arthritis: an in-depth analysis of data from the TOPAS study, Dermatology 212 (3) (2006) 238–249.
- [20] M. Zewail, N.M. El-Deeb, M.R. Mousa, H. Abbas, Hyaluronic acid coated teriflunomide (A771726) loaded lipid carriers for the oral management of rheumatoid arthritis, Int. J. Pharm. 623 (2022) 121939.
- [21] G.P. Thami, G. Garg, Leflunomide in psoriasis and psoriatic arthritis: a preliminary study, Arch. Dermatol. 140 (10) (2004) 1288–1289.
- [22] D. Prosperi, M. Colombo, I. Zanoni, F. Granucci, Drug nanocarriers to treat autoimmunity and chronic inflammatory diseases, Seminars in Immunology, Elsevier (2017).
- [23] M. Zewail, N. Nafee, N. Boraie, Intra-articular dual drug delivery for synergistic rheumatoid arthritis treatment, J. Pharm. Sci. 110 (7) (2021) 2808–2822.
- [24] S. Alivernini, D. Mazzotta, A. Zoli, G. Ferraccioli, Leflunomide treatment in elderly patients with rheumatoid or psoriatic arthritis: retrospective analysis of safety and adherence to treatment, Drugs Aging 26 (2009) 395–402.
- [25] H. Abbas, H.A. Gad, N.S. El Sayed, L.A. Rashed, M.A. Khattab, A.O. Noor, M. Zewail, Development and evaluation of novel leflunomide SPION bioemulsomes for the intra-articular treatment of arthritis, Pharmaceutics 14 (10) (2022) 2005.
- [26] N. Dragicevic-Curic, S. Gräfe, B. Gitter, S. Winter, A. Fahr, Surface charged temoporfin-loaded flexible vesicles: in vitro skin penetration studies and stability, Int. J. Pharm. 384 (1–2) (2010) 100–108.
- [27] M.A. Elgewelly, S.M. Elmasry, N.S. El Sayed, H. Abbas, Resveratrol-loaded vesicular elastic nanocarriers gel in imiquimod-induced psoriasis treatment: in vitro and in vivo evaluation, J. Pharm. Sci. 111 (2) (2022) 417–431.
- [28] M. Zewail, H. Abbas, N. ElSayed, H. Abd-El-Azim, Combined photodynamic therapy and hollow microneedle approach for effective non-invasive delivery of hypericin for the management of imiquimod-induced psoriasis, J. Drug Target. (Just-Accepted) (2024) 1–28.
- [29] S.A. Rizk, M.A. Elsheikh, Y.S.R. Elnaggar, O.Y. Abdallah, Novel bioemulsomes for baicalin oral lymphatic targeting: development, optimization and pharmacokinetics, Nanomedicine 16 (22) (2021) 1983–1998.
- [30] N. Kumar, S. Gupta, A. Dube, S.P. Vyas, Emerging role of vesicular carriers for therapy of visceral leishmaniasis: conventional versus novel, Critical Reviews™ in Therapeutic Drug Carrier Systems 27 (6) (2010).
- [31] X. Zhou, Z. Chen, Preparation and performance evaluation of emulsomes as a drug delivery system for silybin, Arch. Pharm. Res. 38 (12) (2015) 2193–2200.
- [32] R. Kumar, N. Seth, Emulsomes: an emerging vesicular drug delivery system, J. Drug Deliv. Therapeutics 3 (6) (2013) 133–142.
- [33] M.H. Ucisik, U.B. Sleytr, B. Schuster, Emulsomes meet S-layer proteins: an emerging targeted drug delivery system, Curr. Pharm. Biotechnol. 16 (4) (2015) 302, 405
- [34] R. Paliwal, S. Rai, B. Vaidya, K. Khatri, A.K. Goyal, N. Mishra, A. Mehta, S.P. Vyas, Effect of lipid core material on characteristics of solid lipid nanoparticles designed for oral lymphatic delivery, Nanomed.: Nanotech. Bio. Med. 5 (2) (2009) 184–191.
- [35] M.M. Mehanna, R. Sarieddine, J.K. Alwattar, R. Chouaib, H. Gali-Muhtasib, Anticancer activity of thymoquinone cubic phase nanoparticles against human

- breast cancer: formulation, cytotoxicity and subcellular localization, Int. J. Nanomed. 15 (2020) 9557.
- [36] M. Zewail, P.M.E. Gaafar, M.M. Ali, H. Abbas, Lipidic cubic-phase leflunomide nanoparticles (cubosomes) as a potential tool for breast cancer management, Drug Deliv. 29 (1) (2022) 1663–1674.
- [37] H.S. Rahman, A. Rasedee, C.W. How, A.B. Abdul, N.A. Zeenathul, H.H. Othman, M. I. Saeed, S.K. Yeap, Zerumbone-loaded nanostructured lipid carriers: preparation, characterization, and antileukemic effect, Int. J. Nanomed. 8 (2013) 2769.
- [38] M. Zewail, N. Nafee, M.W. Helmy, N. Boraie, Coated nanostructured lipid carriers targeting the joints-an effective and safe approach for the oral management of rheumatoid arthritis, Int. J. Pharm. 567 (2019) 118447.
- [39] S. Ahmed, M.A. Kassem, S. Sayed, Bilosomes as promising nanovesicular carriers for improved transdermal delivery: construction, in vitro optimization, ex vivo permeation and in vivo evaluation, Int. J. Nanomed. 15 (2020) 9783.
- [40] H. Abbas, Y.A. El-Feky, M.M. Al-Sawahli, N.M. El-Deeb, H.B. El-Nassan, M. Zewail, Development and optimization of curcumin analog nano-bilosomes using 21.31 full factorial design for anti-tumor profiles improvement in human hepatocellular carcinoma: in-vitro evaluation, in-vivo safety assay, Drug Deliv. 29 (1) (2022) 714–727.
- [41] M.A. El-Nabarawi, R.N. Shamma, F. Farouk, S.M. Nasralla, Bilosomes as a novel carrier for the cutaneous delivery for dapsone as a potential treatment of acne: preparation, characterization and in vivo skin deposition assay, J. Liposome Res. 30 (1) (2020) 1–11.
- [42] H. Abbas, H. Refai, N. El Sayed, L.A. Rashed, M.R. Mousa, M. Zewail, Superparamagnetic iron oxide loaded chitosan coated bilosomes for magnetic nose to brain targeting of resveratrol, Int. J. Pharm. 610 (2021) 121244.
- [43] H. Abbas, H. Refai, N. El Sayed, Superparamagnetic iron oxide-loaded lipid nanocarriers incorporated in thermosensitive in situ gel for magnetic brain targeting of clonazepam, J. Pharm. Sci. 107 (8) (2018) 2119–2127.
- [44] H. Abbas, N.M. El-Deeb, M. Zewail, PLA-coated Imwitor® 900 K-based herbal colloidal carriers as novel candidates for the intra-articular treatment of arthritis, Pharm. Dev. Technol. 26 (6) (2021) 682–692.
- [45] A.L. Onugwu, A.A. Attama, P.O. Nnamani, S.O. Onugwu, E.B. Onuigbo, V. V. Khutoryanskiy, Development and optimization of solid lipid nanoparticles coated with chitosan and poly (2-ethyl-2-oxazoline) for ocular drug delivery of ciprofloxacin, J. Drug Delivery Sci. Technol. 74 (2022) 103527.
- [46] V.V. Yuzhakov, Microneedle array, patch, and applicator for transdermal drug delivery, https://patents.google.com/patent/WO2007081430A3/en, 2010.
- [47] V.V. Yuzhakov, The AdminPen™ microneedle device for painless & convenient drug delivery, Drug Deliv. Tech. 10 (4) (2010) 32–36.
- [48] E. Larrañeta, J. Moore, E.M. Vicente-Pérez, P. González-Vázquez, R. Lutton, A. D. Woolfson, R.F. Donnelly, A proposed model membrane and test method for microneedle insertion studies, Int. J. Pharm. 472 (1–2) (2014) 65–73.
- [49] E. Abd, S.A. Yousef, M.N. Pastore, K. Telaprolu, Y.H. Mohammed, S. Namjoshi, J. E. Grice, M.S. Roberts, Skin models for the testing of transdermal drugs, Clin. Pharmacol.: Adv. Appl. 8 (2016) 163.
- [50] M. Jabeen, A.-S. Boisgard, A. Danoy, N. El Kholti, J.-P. Salvi, R. Boulieu, B. Fromy, B. Verrier, M. Lamrayah, Advanced characterization of imiquimod-induced psoriasis-like mouse model, Pharmaceutics 12 (9) (2020) 789.
- [51] Y.-K. Lin, S.-H. Yang, C.-C. Chen, H.-C. Kao, J.-Y. Fang, Using imiquimod-induced psoriasis-like skin as a model to measure the skin penetration of anti-psoriatic drugs, PLoS One 10 (9) (2015) e0137890.
- [52] T. Chen, L.X. Fu, Z.P. Guo, B. Yin, N. Cao, S. Qin, Involvement of high mobility group box-1 in imiquimod-induced psoriasis-like mice model, J. Dermatol. 44 (5) (2017) 573–581.
- [53] I. Flisiak, P. Porebski, B. Chodynicka, Effect of psoriasis activity on metalloproteinase-1 and tissue inhibitor of metalloproteinase-1 in plasma and lesional scales, Acta Derm. Venereol. 86 (1) (2006).
- [54] A. Goldminz, S. Au, N. Kim, A. Gottlieb, P. Lizzul, NF-κB: an essential transcription factor in psoriasis, J. Dermatol. Sci. 69 (2) (2013) 89–94.
- [55] N. Starodubtseva, V. Sobolev, A. Soboleva, A. Nikolaev, S. Bruskin, Genes expression of metalloproteinases (MMP-1, MMP-2, MMP-9, and MMP-12) associated with psoriasis, Russ. J. Genet. 47 (2011) 1117–1123.
- [56] A. Rendon, K. Schäkel, Psoriasis pathogenesis and treatment, Int. J. Mol. Sci. 20 (6) (2019) 1475.
- [57] E. Campione, S. Mazzilli, M. Di Prete, A. Dattola, T. Cosio, D. Lettieri Barbato, G. Costanza, C. Lanna, V. Manfreda, R. Gaeta Schumak, F. Prignano, The role of glutathione-S transferase in psoriasis and associated comorbidities and the effect of dimethyl fumarate in this pathway, Front. Med. 9 (2022).
- [58] A. Myers, R. Lakey, T. Cawston, L. Kay, D. Walker, Serum MMP-1 and TIMP-1 levels are increased in patients with psoriatic arthritis and their siblings, Rheumatology 43 (3) (2004) 272–276.
- [59] G. Drewa, E. Krzyzyńska-Malinowska, A. Woźniak, F. Protas-Drozd, C. Mila-Kierzenkowska, M. Rozwodowska, B. Kowaliszyn, R. Czajkowski, Activity of superoxide dismutase and catalase and the level of lipid peroxidation products reactive with TBA in patients with psoriasis, Med. Sci. Monitor: Int. Med. J. Exp. Clin. Res. 8 (8) (2002) BR338-43.
- [60] V.N. Sehgal, P. Verma, Leflunomide: dermatologic perspective, J. Dermatol. Treat. 24 (2) (2013) 89–95.